Available online at www.sciencedirect.com
SCIENCE DIRECT
Journal of Physiology - Paris 98 (2004) 498–506
Journal of Physiology Paris
www.elsevier.com/locate/jphysparis

Comparing information about arm movement direction in single channels of local and epicortical field potentials from monkey and human motor cortex

Carsten Mehring [a,b,*,1], Martin Paul Nawrot [a,b,c,1], Simone Cardoso de Oliveira [b,d], Eilon Vaadia [e], Andreas Schulze-Bonhage [b,f], Ad Aertsen [b,c], Tonio Ball [b,f,1]

[a] *Institute for Biology I, Hauptstr. 1, Albert-Ludwigs-University, 79104 Freiburg, Germany*
[b] *Berstein Center for Computational Neuroscience, Albert-Ludwigs-University, 79104 Freiburg, Germany*
[c] *Institute for Biology III, Schänzlestr. 1, Albert-Ludwigs-University, 79104 Freiburg, Germany*
[d] *German Primate Center, Kellnerweg 4, 37077 Göttingen, Germany*
[e] *Department of Physiology and the Interdisciplinary Center for Neural Computation, The Hebrew University, Hadassah Medical School, POB 12272, Jerusalem 91120, Israel*
[f] *Epilepsy Center, University Clinics, Albert-Ludwigs-University, Hugstetter Straße 49, 79095 Freiburg, Germany*

Abstract

Cortical field potentials have been used for decades in neurophysiological studies to probe spatio-temporal activity patterns of local populations of neurons. Recently, however, interest in these signals was spurred as they were proposed as potential control signals for neuronal motor prostheses, i.e., for devices fit to record and decode brain activity to restore motor functions in paralyzed patients. Little is known, however, about the functional significance of these cortical field potentials. Here we compared information about arm movement direction in two types of movement related cortical field potentials, obtained during a four direction center-out arm reaching paradigm: local field potentials (LFPs) recorded with intracortical micro-electrodes from monkey motor cortex, and epicortical field potentials (EFPs) recorded with macro-electrode arrays subdurally implanted on the surface of the human cerebral cortex. While monkey LFPs showed a typical sequence of positive and negative potential peaks, an initial negative peak was the most salient feature of human EFPs. Individual contralateral LFPs from the monkey motor cortex carried approximately twice as much decoded information (DI) about arm movement direction (median 0.27 bit) as did individual EFPs from the contralateral hand/arm area of primary motor cortex in humans (median 0.12 bit). This relation was similar to the relation between median peak signal-to-noise ratios for directional modulation of movement related potentials (MRPs) of both types of signals. We discuss possible reasons for the observed differences, amongst them epi- vs. intracortical recording and the different electrode dimensions used to measure EFPs and LFPs.

Keywords: Neuronal signal types; Subdural electrodes; Brain–machine interface; Movement decoding; Motor control

1. Introduction

A much debated question in current brain–machine interface (BMI) research is which neuronal signal (or combination of signals) is optimal for controlling neuronal motor prostheses. In addition to the electroencephalogram (EEG) derived from the scalp surface [6,7,26,41,42] and single neuron activity (SUA) recorded intracortically [10,35,37], two forms of neuronal population activity have recently been proposed as BMI control signals: local field potentials (LFPs) measured with penetrating, intracortical electrodes [22,25,29,32], and epicortical field potentials (EFPs) measured with non-penetrating electrodes placed directly on the brain surface [2,3,18,19,21].

* Corresponding author.
E-mail address: mehring@biologie.uni-freiburg.de (C. Mehring).
[1] These authors contributed equally to this work.

0928-4257/$ - see front matter © 2005 Elsevier Ltd. All rights reserved.
doi:10.1016/j.jphysparis.2005.09.016

Investigating eye movement related LFP activity in monkey parietal cortex, Pesaran et al. [25] reported that LFP oscillations in the gamma range can be used to differentiate between two possible saccade directions.

In [22] we showed that the low-frequency component of the LFP signal recorded from monkey motor cortex can be used to accurately infer the direction of arm movements (Fig. 1). Moreover, eight simultaneously recorded LFPs allowed for the approximate prediction of arm movement trajectories. Single-trial inference based on LFPs was found to be as efficient as inference based on multiple SUA. By combining SUA and LFPs, an even higher accuracy was obtained than by using either SUA or LFP recordings alone. Interestingly, recent results indicate that also LFP activity in the gamma range contains directional information about arm movements [29]. In summary, these studies show that LFPs contain substantial information about details of voluntary arm movements.

A potential use of EFPs recorded with subdural electrodes for BMIs was investigated in a number of recent studies in epilepsy patients undergoing pre-neurosurgical diagnostics. Levine et al. [19] described an approach where temporal signal templates corresponding to specific movement types (e.g., wrist extension, tongue protrusion) were first constructed from trigger-averaged signals. Then, a running template matching was used to detect the prototypes in continuous recordings. Recently, the detection performance was shown to increase when applying wavelet analysis, taking into account not only the mean evoked potentials dominated by low frequencies, but also higher frequency components in the alpha, beta and gamma range [16]. Thus, reliably detected movement types could be used for binary decision steps. Subdural recordings from epilepsy patients were also successfully used to achieve closed-loop control with success rates of 74–100% in a one-dimensional binary decision task [18]. In contrast to the continuous detection approach, the latter experiments were based on classification of activity (for instance hand movement) vs. inactivity within a predefined time window.

For an effective control of a neuronal motor prosthesis, however, accurate single-trial decoding of parameters of more complex voluntary movements will be necessary. In an ongoing project, we are investigating the potential of decoding parameters of voluntary movement from EFPs measured from cerebral motor areas, adopting a similar approach as we used for decoding LFPs from monkey motor cortex [22,29,32]. We could demonstrate that the low-frequency component of multiple EFPs simultaneously recorded from frontal cortex is suitable for accurate inference of arm movement direction on a single-trial basis [21]. Primary motor cortex was found to be the principal source of directional information within the frontal cortex. In the study of Leuthardt et al. [18], there is also evidence for arm movement related directional information in gamma band EFP activity. There, however, with separate training and test data sets, in two of three subjects the correlation of actual and predicted movement target coordinates was rather low for both x and y coordinates (r^2 0.02–0.1). Moreover, the location of the cortical generators of this specific gamma response (motor or somatosensory cortex?) needs further investigation.

The main objective of the present study was to compare the efficacy of inferring the direction of arm movements, using the identical decoding algorithm, from LFPs and EFPs obtained during a classical center-out reaching movement task. First, the nature of and the relation between different types of cortical field potentials is of principal interest, especially to bridge the gap between localized populations of neurons as measured by the LFP and neuronal mass signals as typically measured, for example, with surface EEG, magnetoencephalography (MEG) or functional magnetic resonance imaging (fMRI), surface EEG, or magnetencephalography (MEG). Second, this study was also

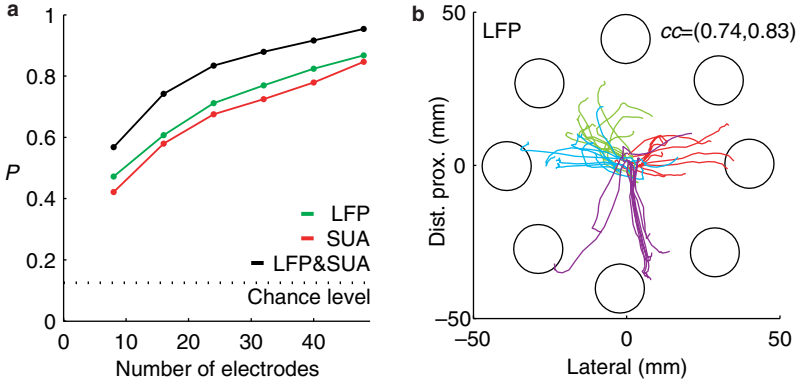

Fig. 1. Decoding of movement target and trajectories from multiple local field potentials (LFP). (a) Average probability of correctly discriminating between eight targets as a function of the number of recording electrodes. LFPs (green) and single-unit activity (SUA, red), both recorded simultaneously from identical sets of micro-electrodes yielded a similar decoding power. Using LFPs in conjunction with simultaneously recorded SUAs (black) further increased the average decoding power. (b) Examples of hand trajectories to four different targets predicted from eight simultaneously recorded LFP channels. The linear correlation coefficient (cc) between predicted and real trajectories is given for lateral- and distal-proximal axis separately. (Modified and reprinted from [22] by kind permission of Nature Publishing Group, London, UK.)

motivated by the question how EFP recordings may be optimized for BMI applications. In this context, it is crucial to know how LFP- and EFP-performance compares under similar task conditions. To address these issues, we decoded single channels of LFPs and EFPs, quantified the decoding efficacy by the probability of correctly inferring movement direction (decoding power, DP) and the amount of decoded information (DI), and compared the results in the two cases.

2. Materials and methods

2.1. Recording epicortical field potentials in humans

Three patients (S1–S3) suffering from intractable pharmacoresistant epilepsy took part in this study after having given their informed consent. The study was approved by the University Clinic's ethics committee. The subjects were 70–100% right-handed after a modified Oldfield questionnaire [23] and showed no clinical signs of pareses or other movement disorders. Platinum electrode arrays (4 mm electrode diameter, 2.3 mm exposure, $<2\,k\Omega$ impedance at 64 Hz) were subdurally implanted above the left (S1,S2) resp. right (S3) lateral fronto-parieto-temporal regions for pre-neurosurgical diagnostics (Fig. 2). In two subjects (S1,S2) the electrode array had 112 contacts with 7.1 mm inter-electrode distance, in the third subject (S3) the electrode array had 64 contacts with 10 mm inter-electrode distance.

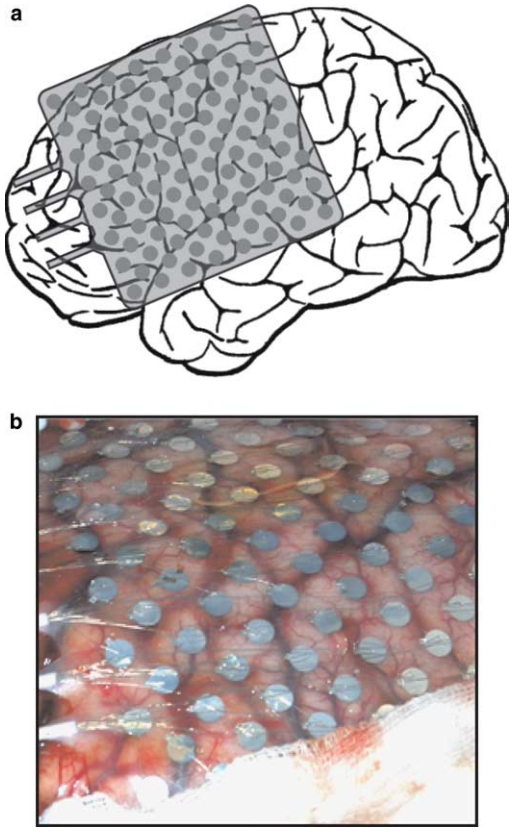

Fig. 2. Subdurally implanted electrode grid. (a) Approximate location of the 112 contact electrode array over the left cerebral hemisphere of subject S1, covering part of the prefrontal, premotor, primary motor, parietal, and temporal cortex. (b) Intraoperatively taken photograph of subdural electrode array electrode implantation in S2.

The subjects were instructed to perform a center-out arm reaching task with the arm contralateral to the implantation side in four directions (right, left, forward, backward) starting from a central position (target distance from center 20 cm). Movements were self-paced with inter-trial intervals of at least 4 s. Electrocorticograms (ECoGs) were band-pass filtered (0.032–97 Hz) and digitized at either 256 Hz (S1,S3) or 512 Hz (S2) using a clinical AC EEG-System (IT-Med, Germany). Onset and offset of arm movements were determined based on digital video (25 Hz sampling rate) synchronized to the ECoG. The movement durations were $1.0\,s \pm 0.3\,s$ (S1), $0.9\,s \pm 0.1\,s$ (S2) and $1.0\,s \pm 0.1\,s$ (S3), respectively.

Electrical stimulation was performed with stimulator INOMED NS60 (INOMED, Germany) to demarcate the motor and somatosensory brain areas. The intensity of stimulation was gradually increased up to 15 mA or to the induction of sensory and motor phenomena. All sites with arm or hand motor responses were located outside the ictal onset zone.

A structural MRI data set with full head coverage was acquired on the day after electrode implantation using a T1 MPRAGE sequence. The exact relation of the individual electrode contacts to the cortical anatomy was determined using curvilinear reconstructions [34]. The motor cortices were identified according to anatomical landmarks (for references see [4]). The border between premotor (PM) and prefrontal cortex was defined on the basis of the location of the frontal eye field, the extent of PM as described in the anatomical literature (e.g., [15]), and such that PM included all electrode contacts outside the primary motor cortex with motor responses. Electrodes with eye motor responses or upper extremity sensory responses were excluded from the frontal electrode groups.

2.2. Recording local field potentials in monkeys

The experimental procedures were described in detail in previous publications [9,14]. Briefly, two monkeys (*Macaca mulatta*) were trained to use two manipulanda (one with each arm) which each controlled a cursor on a vertically oriented screen. Here, we used neuronal activity recorded when the monkeys performed unimanual center-out movements with either the right or the left arm in response to a visual cue. All movements started from a central resting position and ended in one of eight targets, regularly arranged on a circle around the resting position. The movement duration was 0.6 ± 0.1 for both monkeys. Single-unit activity and local field potentials were recorded by eight micro-electrodes (0.2–0.8 MΩ impedance at 1 kHz) from homologous sites in the two hemispheres (four electrodes in each hemisphere). In this study we used the same data as in [22] but analyzed exclusively the LFPs (low-pass filtered with a cut-off frequency of 150 Hz and digitized at 400 Hz) and studied only the four movement directions corresponding to those performed in the human task. The animals' care and surgery procedures were in accordance with *The NIH Guide for the Care and Use of Laboratory Animals* (revised 1996) and the Hebrew University regulations.

2.3. Computation of movement related potentials and power spectra

To extract the low-frequency movement related potentials (MRPs) we smoothed the raw signals. EFP recordings were filtered with a second order Savitzky–Golay filter of 141 or 281 bins width for S1, S3 (256 Hz sampling rate) and S2 (512 Hz sampling rate), respectively. LFP recordings were filtered with a second order Savitzky–Golay filter of 63 bins width. For visualization of epicortical MRPs we subtracted a baseline obtained by averaging the activity in the window from 2000 ms to 1000 ms before movement onset.

Power spectra of epicortical field potentials were calculated for each trial individually with a frequency resolution of 2 Hz by multi-taper methods [24,38] using three prolate spheroidal data tapers and a window from 0 ms to 500 ms after movement onset. To analyze the relative power

changes during movement, we normalized the power spectra for each frequency bin by the baseline power obtained in the window from 2000 ms to 1500 ms before movement onset.

2.4. Computation of signal-to-noise ratio of directional modulation

As a measure of the strength of directional modulation of MRPs we computed the signal-to-noise ratio (SNR) for each point in time. The SNR was defined as the variance of the directional modulation divided by the variance of the trial-by-trial fluctuations and was computed as described in [22].

2.5. Decoding of movement related potentials

Both for epicortical and local field potentials we decoded the movement related potentials using the time window from movement start to movement end. Decoding on a single-trial basis was performed by using penalized linear discriminant analysis [17]. To calculate the probability of correct decoding (termed *decoding power*, *DP*) we performed leave-one-out cross-validation [8]. Thus, trials used to train the classification algorithm were not included in the test set for decoding.

2.6. Information theoretic analysis

To quantify the extracted information about movement direction decoded from field potentials, we computed the Shannon mutual information [11] between the decoded movement targets and the real movement targets:

$$I(T_D;T)=\sum_{t_D\in T_D}\sum_{t\in T}p(t_D,t)\log_2\left[\frac{p(t_D,t)}{p(t_D)p(t)}\right]$$

where T_D denotes the set of decoded targets $\{t_D\}$, T denotes the set of real targets $\{t\}$, $p(t_D,t)$ denotes the joint probability distribution of decoded and real targets, and $p(t_D)$, $p(t)$ denote the marginal probability distributions of decoded and real targets. In the following, we termed this information quantity the *decoded information* (*DI*). The data processing inequality (e.g., [11]) implies that DI yields a lower bound on the mutual information between the field potential and the movement target.

In general, the estimation of mutual information from limited experimental data is biased. We used the approach of Treves and Panzeri [40] to correct for this sampling bias.

The decoding power is given by the trace of the joint probability distribution $p(t_D,t)$:

$$DP=\sum_{\substack{t\in T\\ t_D=t}}p(t_D,t)$$

For each DP value multiple $p(t_D,t)$ and multiple DI values exist. To determine the relation between DP and DI we used the following numerical procedure: We assumed 20 trials per target, making DP values between 0 and 1 in steps of 0.0125 possible. For each DP value we randomly chose 1000 joint probability distributions $p(t_D,t)$ and computed their DI (incl. bias correction) as described above. A scatter plot of these 81,000 pairs of (DP,DI) values is shown in Fig. 7c.

3. Results

A topographic map of trial-averaged movement related potentials (MRPs) shortly (250 ms) after movement onset is shown in Fig. 3a. In this example, a surface negative potential above the motor cortex can be distinguished from a surface-positive potential in the inferior parietal cortex, similar to the results of Satow et al. [31] also obtained during simple movement tasks. Movement related changes of relative spectral power for the alpha/beta (8–30 Hz) band and an intermediate-to-high (50–128 Hz) part of the gamma band are shown in Fig. 3b and c, respectively. The decrease in the alpha/beta power corresponds to the classical movement related 'desynchronization' described for the alpha/beta band, and the increase in the gamma power to the so-called movement related 'synchronization' [28].

Here, for decoding movement direction we exclusively used the low-frequency component of the MRPs in both, human EFP and monkey LFP. Fig. 4a illustrates the time course of this signal component for all electrode contacts localized above the hand/arm area of the primary motor cortex (M1), pooled from all three subjects. Responses were quite variable, a negative peak during the initial phase of movement execution was the most reproducible feature across channels and subjects. By comparison, Fig. 4b displays the trial-averaged LFP time course for 10 randomly selected electrodes placed in M1 contralateral to the side of movement. Note that the durations of the reaching movements performed by the monkeys were approximately half as long as those of the human subjects (cf. Sections 2.1 and 2.2).

Mean LFPs and EFPs for each direction are shown exemplarily in Fig. 5a and b. Strong directional modulation

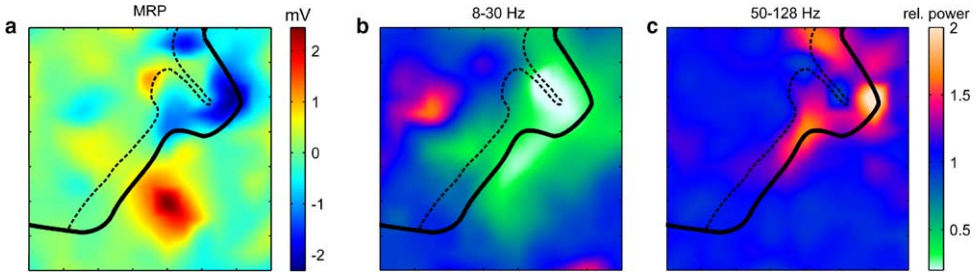

Fig. 3. Movement related potentials 250 ms after movement onset (a), relative spectral power changes for the alpha/beta band (b) and gamma band (c) in the time window of 0–500 ms after movement onset, relative to the baseline 2000–1500 ms before movement onset. Each plot corresponds to the square area covered by the complete electrode array as shown in Fig. 2a. The solid black line indicates the border of the frontal lobe defined by the central and lateral sulci, the dashed black line marks the border between M1 and PM defined by the precentral sulcus. Note the widespread depression of power in the alpha/beta band (green and white area in b) and the more focal power increase in the gamma band (red area in c), corresponding to the classical so-called movement related 'desynchronization' resp. 'synchronization' [28]. Averaged data of subject S1 over all four movement directions, maps interpolated.

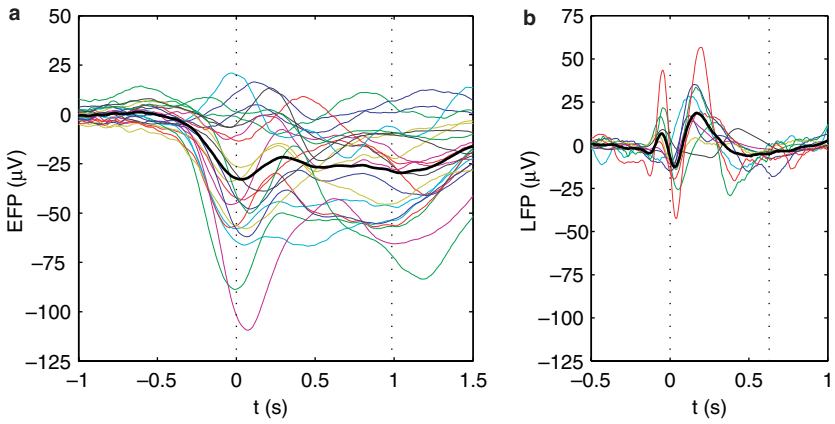

Fig. 4. Movement related potentials (MRPs). (a) Each curve represents a single channel EFP averaged across all trials irrespective of movement direction. Shown are all 23 channels from all three subjects that were positioned over the hand/arm area of the primary motor cortex. Black line shows the grand mean. (b) Trial-averaged LFPs from 10 randomly chosen electrodes in the hand/arm area of M1 from two monkeys. The grand mean (black) resembles the characteristic multiphasic features found in many single channels. The dotted lines denote the time of movement onset and the times of movement end.

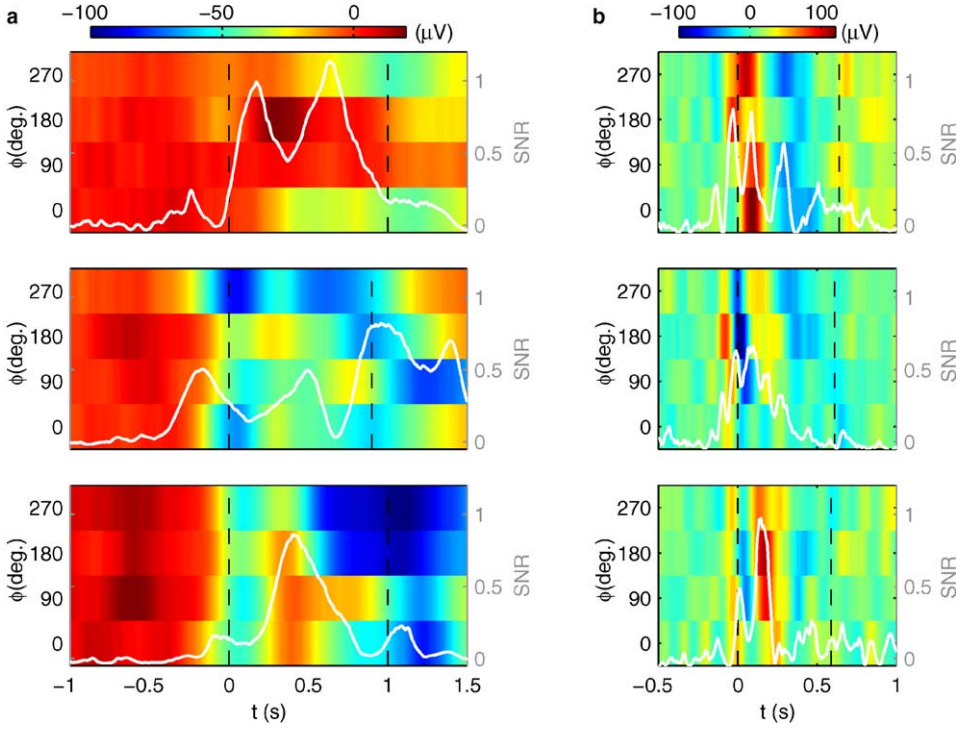

Fig. 5. Directional modulation of movement related potentials (MRPs) in single channel human EFP (a) and monkey LFP (b). The dashed lines denote the time of movement onset and the times of movement end. All examples were recorded from the hand/arm area of the motor cortex of the precentral gyrus. Trial-averaged potentials were calculated separately for the four movement directions from 1 s before to 1.5 s after movement onset (a), resp. from 0.5 s before to 1 s after movement onset (b). Direction of movement φ in degrees is assigned to the left ordinate, $\varphi = 0°$ corresponds to rightward movement; φ increases counter-clockwise, i.e., 90° corresponds to forward movement. White curves show the time course of the signal-to-noise ratio (SNR, see Methods). EFP examples represent channels with high SNR from all three subjects (S1, S2, S3 from top to bottom). LFP examples represent channels with peak SNR from the upper third of the peak SNR distribution. For a comparison of the complete distributions of the peak SNR of EFPs and LFPs see Fig. 6.

was seen in the time period of movement execution. Time-resolved SNR is shown as white curves. Its peaks corresponded well to the times where directional differences in the color coded mean activity were most pronounced.

We computed the signal-to-noise ratio (SNR) of the directional modulation of both LFPs and EFPs, and decoded individual EFPs recorded from human motor cortex and individual LFPs from monkey motor cortex on a single-trial basis. In addition to decoding power (DP), we quantified the decoded information (DI) for the single LFP/EFP channels (see Methods for both measures). In Fig. 6, the distribution of the peak signal-to-noise ratio,

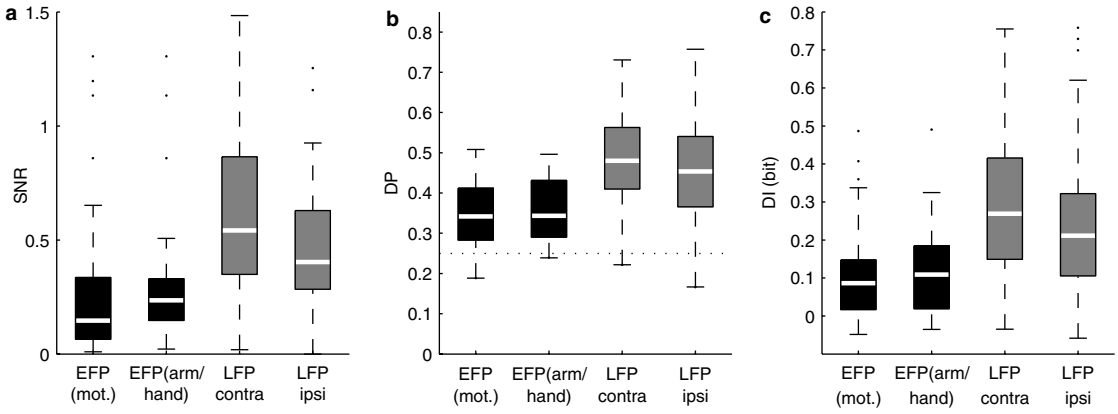

Fig. 6. Strength of directional modulation of EFPs and LFPs. (a) Distributions of the peak signal-to-noise ratio (SNR) during the movement phase for 65 electrodes above motor cortex, pooled from all three subjects (left black) and the subset of 22 electrodes above the hand/arm areas of M1 (right black). SNR of single channel LFPs ($N = 74$), pooled from two monkeys, are shown separately for contralateral (left gray) and ipsilateral (right gray) movement. (b) Corresponding distributions of decoding power (DP) and (c) of decoded information (DI). Dotted line in (b) depicts chance level of 0.25. Box plots show distributions with white lines indicating the median, box margins denoting the lower and upper quartiles, and the whiskers extending from the box out to the most extreme data values within 1.5 times the inter-quartile range.

the decoding power, and the decoded information is given separately for different groups of EFP and LFP channels.

The distribution of DP was clearly above chance level (0.25) both for contra-/ipsilateral LFPs and for EFPs recorded from the contralateral motor cortex (Fig. 6b, note that no ipsilateral EFPs were recorded for the present study). Motor cortical EFPs yielded a median DP of 0.34, the EFPs recorded from the hand/arm area of M1 yielded a slightly higher median DP of 0.37. By comparison, the median decoding power of LFPs was 0.49 and 0.45 for contra- and ipsilateral recordings, respectively. Thus, the DP of LFPs was substantially higher than the DP of EFPs. In addition, the distribution of DP of LFPs was broader than the distribution of DP of EFPs, and maximal DP values of 0.78 and 0.50 were observed for LFPs and EFPs, respectively. The distributions of the DI (Fig. 6c) for the different neuronal signals confirmed that contralateral LFPs contained most directional information (median 0.27 bit), followed by ipsilateral LFPs (median 0.21 bit), EFPs from the hand/arm area of M1 (median 0.12 bit) and motor cortical EFPs (median 0.09 bit). Therefore, contralateral LFPs carried approximately twice as much information about movement direction as contralateral EFPs. The order of median peak SNR (Fig. 6a) confirmed the order found in DP (Fig. 6b) and DI (Fig. 6c). Furthermore, a clear relation between peak SNR and DI was found for both LFPs and EFPs (Fig. 7a).

We calculated numerically (see Methods) the relation between DP and DI for the full range of DP and DI values (Fig. 7b). The relationship between DP and DI is non-linear and also non-unique, except for the case where $DP = 1$, which coincides with maximal DI. In general, a range of different DP values may correspond to the same DI, and vice versa. In the mean, DI rises monotonically with DP for DP values above chance level (0.25). The relation between DP and DI for the measured LFP/EFP data

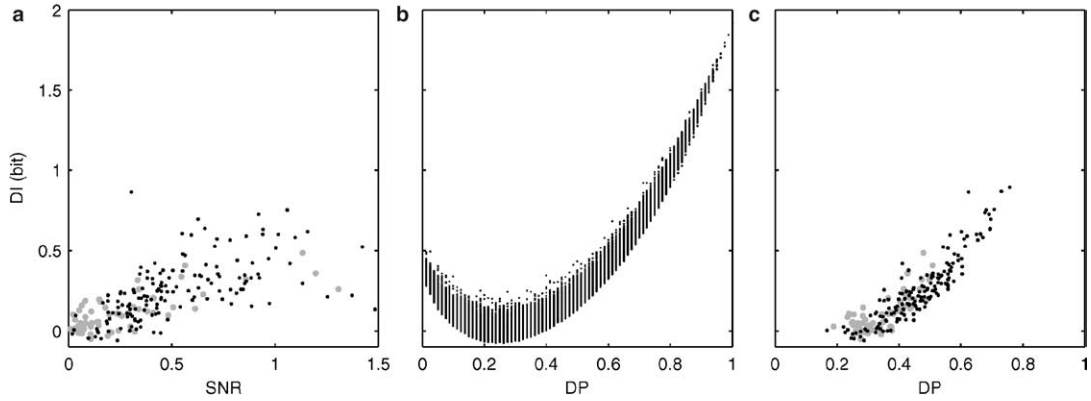

Fig. 7. Relation between peak SNR, decoding power (DP) and decoded information (DI). (a) Relation between peak SNR and DI for EFPs (large gray dots) and LFPs (small black dots). (b) Relation between DP and DI as determined numerically. The relationship between DP and DI is non-linear and also non-unique, except for the case of $DP = 1$, which coincides with maximal DI. Everywhere else, a range of different DP values may correspond to the same DI, and vice versa. (c) Relation between DP and DI for EFPs (large gray dots) and LFPs (small black dots).

(Fig. 7c) was consistent with the numerically obtained relation.

It should be noted that we discriminated here only between four different movement directions in the LFPs to allow direct comparison of monkey and human experimental data. We showed in [22] that for eight movement directions the average decoding power of the same LFP channels shown in Fig. 6 is 0.25 and 0.21 for contra- and ipsilateral recordings.

4. Discussion

In the present study we compared the efficacy of inferring the direction of arm movements from LFPs and EFPs, recorded from monkey and human motor cortex, respectively. As previously described in detail by Donchin et al. [13], monkey LFPs exhibited a characteristic time course during voluntary arm movements, with a sequence of positive and negative potential peaks (see also Fig. 4b). To our knowledge, only two previous studies [18,39] have presented data from subdurally implanted electrodes obtained during arm movement. In both, however, mean MRPs were not documented and, thus, the characteristics of human EFPs during arm movements are not known. Our results show one salient characteristic of these potentials: a negative peak during the initial phase of movement execution was the most reproducible feature across channels and subjects (Fig. 4a). Note, that while the movement duration was about half as large for monkeys, also the duration of the evoked potentials scaled with a similar factor.

In both LFPs [25,30] and EFPs [3,16,18,27], movement related changes involve multiple frequency bands (see also Fig. 3). In the present study we analyzed the LFP and EFP low-frequency components only. Previously, we had found both suitable for accurate single-trial inference of arm movement direction [21,22], EFPs also appear promising for decoding finger movement related information [3]. However, there is also evidence for directional information about eye and arm movements in gamma band activity of LFPs recorded from monkey [25,29] and EFPs recorded from human cortex [18].

Here, we have decoded field potentials occurring during movement execution. From the work of Shoham et al. [36] there is evidence that attempts to move a paralyzed limb result in a similar macroscopic activation pattern in human motor cortex as do real movements of the same limb in healthy subjects. Furthermore, observations in cord-transected baboons suggest that there are persistent epicortical potentials during the attempt to move a limb [12]. Thus, paralyzed subjects attempting to move might indeed be able to generate field potentials similar to the movement related epicortical potentials we measured during the execution of movements and used for decoding. Alternatively, also pre-movement or movement-imagery-related potentials might be used for BMI applications. Which of these signals is most suited for neuro-prosthetic control is still open at this point.

Generally, different measures may be used to assess the quality of decoding of behavioral parameters. We used two such measures, decoding power (DP) and decoded information (DI). We obtained consistent results for both, showing that the average accuracy of inference of arm movement direction is significantly higher for LFPs recorded from monkey motor cortex than for EFPs recorded from human motor cortex. Single channels of contralateral LFPs carried approximately twice as much information about movement direction as single channels of contralateral EFPs from hand/arm area of M1. Even the DI of ipsilateral LFPs was higher than the DI of contralateral EFPs, although the difference was less pronounced than between contralateral LFPs and contralateral EFPs. The difference between contra- and ipsilateral LFPs may be explained by the pre-dominant role of the contralateral motor cortex, especially in the control of voluntary arm and hand movements. It has to be mentioned, though, that the decoding power of single channels of EFPs and LFPs, as analyzed here, may not be sufficient for practical BMI purposes, but multiple channels can yield a much higher decoding accuracy EFPs [2,21].

Which aspect of the analyzed signals may explain the considerable difference between LFPs and EFPs? As shown in Fig. 6, the order of median peak SNR (Fig. 6a), median DP (Fig. 6b), and median DI (Fig. 6c) across the different signal types was identical. This indicates that the directional modulation of the trial-averaged MRPs, the strength of which is measured by the SNR, captures the main source of the differences in decoding quality of individual LFPs and EFPs. By contrast, more complex effects such as movement direction specific differences in the distribution of MRPs not seen in the mean potentials, or synergy/redundancy effects between different time points of the signal, appear to play a minor role in explaining our results.

The stronger directional modulation of LFPs over EFPs may, in turn, reflect a number of differences: LFPs were measured intracortically in deeper layers while EFPs were recorded on the cortical surface, possible species differences between human and monkey motor cortex (e.g., [33]), differences in movement task (externally triggered in monkeys, self-paced in humans) and movement duration (about half as long in monkeys as in humans), and/or differences in the exact subdivisions of precentral motor cortex from which the respective recordings were made. Also the quite different types of electrodes used for recording LFPs resp. EFPs may have accounted for the different behaviour of LFPs and EFPs: LFPs were recorded with intracortical sharp electrodes of 1–2 μm tip diameter, increasing to 50 μm on a length of 10–40 μm, with an impedance of 0.2–0.8 MΩ at 1 kHz. EFPs were measured with subdurally implanted arrays of planar surface electrodes, consisting of contact discs of 4 mm diameter, 2.3 mm exposure and with an impedance below 2 kΩ at 64 Hz, placed directly on the brain surface. Thus, due to their larger size and shape, the electrodes used to record

EFPs pick up currents from a larger volume of tissue than the micro-electrodes used for the LFP recordings.

Both aspects (intra- vs. epicortical and micro- vs. macro-electrodes) may profoundly influence the nature and composition of the recorded neuronal signals. For instance, there is increasing evidence for some spatial order map of tuning properties of single neurons in M1 [1,5,20]. Amirikian and Georgopoulos [1] found cells with similar tuning properties segregated into vertically oriented minicolumns 50–100 μm in width. Parallel to the cortical layers, minicolumns with similar preferred directions (PDs) were about 200 μm apart and minicolumns with nearly opposite PDs were approximately 350 μm apart. Thus, signals from minicolumns representing nearly opposite PDs would be expected to partially cancel out each other when using large electrodes, presumably measuring a compound signal arising from neuronal populations comprising many such minicolumns. On the other hand, signals from different cortical depth resp. layers might possibly be more or less suitable for extraction of movement related information. On the basis of these considerations we conclude that it would be highly desirable to identify whether the better decoding performance of individual LFPs compared to EFPs is mainly due to the smaller electrode size and/or to the difference in recording depth.

In a complementary study (manuscript in preparation) we investigated the role of electrode spacing in decoding information about arm movement direction in the LFP and EFP recordings analyzed here. There, signal relations and directional information were analyzed to probe at which spatial scale the information content of LFPs and EFPs became highly redundant. We found a statistically significant, substantial gain of decoded information for simultaneously recorded EFPs from densely spaced electrodes above motor cortex, even for the smallest inter-electrode distance of 7.1 mm. In the LFPs, a substantial gain of decoded information was still present at an inter-electrode distance of 350–700 μm. These findings show that, along with electrode size, also spatial sampling density of cortical field potentials should be further evaluated for optimally recording and decoding cortical surface activity.

In summary, further comparisons of BMI approaches based on different neuronal signals are important for developing optimized neuronal motor prostheses in humans. Moreover, they will help us to improve our still relatively poor insight into the neural basis of cortical field potentials. Insight from such studies may provide a conceptual bridge between microscopic and macroscopic aspects of cortical dynamics.

Acknowledgements

We thank Dr. J. Honegger for providing the photograph used in Fig. 2b. This work was supported by the WIN-Kolleg of the Heidelberg Academy of Sciences and Humanities and the German Federal Ministry of Education and Research (BMBF-DIP and BMBF grant 01GQ0420).

References

[1] B. Amirikian, A.P. Georgopoulos. Modular organization of directionally tuned cells in the motor cortex: is there a short-range order? Proc. Natl. Acad. Sci. USA 100 (2003) 12474–12479.
[2] C. Mehring, M.P. Nawrot, A. Schulze-Bonhage, A. Aertsen, T. Ball, Human brain–machine interfacing based on epicortical field potentials: Comparison of different decoding methods, Biomed. Eng. (Berlin) 50 (Suppl. 1(1)) (2005) 536–537.
[3] T. Ball, M.P. Nawrot, T. Pistohl, A. Aertsen, A. Schulze-Bonhage, C. Mehring, Towards an implantable brain–machine interface based on epicortical field potentials, Biomed. Tech. (Berlin) 49 (Suppl. 2) (2004) 756–759.
[4] T. Ball, A. Schreiber, B. Feige, M. Wagner, C.H. Lucking, R. Kristeva-Feige, The role of higher-order motor areas in voluntary movement as revealed by high-resolution EEG and fMRI, Neuroimage 10 (1999) 682–694.
[5] Y. Ben Shaul, E. Stark, I. Asher, R. Drori, Z. Nadasdy, M. Abeles, Dynamical organization of directional tuning in the primate premotor and primary motor cortex, J. Neurophysiol. 89 (2003) 1136–1142.
[6] N. Birbaumer, N. Ghanayim, T. Hinterberger, I. Iversen, B. Kotchoubey, A. Kubler, J. Perelmouter, E. Taub, H. Flor, A spelling device for the paralysed, Nature 398 (1999) 297–298.
[7] B. Blankertz, G. Dornhege, C. Schafer, R. Krepki, J. Kohlmorgen, K.R. Muller, V. Kunzmann, F. Losch, G. Curio, Boosting bit rates and error detection for the classification of fast-paced motor commands based on single-trial EEG analysis, IEEE Trans. Neural Syst. Rehabil. Eng. 11 (2003) 127–131.
[8] E. Bradley, R.J. Tibshirani, An Introduction to the Bootstrap, Chapman & Hall/CRC Press LLC, 1998.
[9] S. Cardoso de Oliveira, A. Gribova, O. Donchin, H. Bergman, E. Vaadia, Neural interactions between motor cortical hemispheres during bimanual and unimanual arm movements, Eur. J. Neurosci. 14 (2001) 1881–1896.
[10] J.M. Carmena, M.A. Lebedev, R.E. Crist, J.E. O'Doherty, D.M. Santucci, D. Dimitrov, P.G. Patil, C.S. Henriquez, M.A. Nicolelis, Learning to control a brain–machine interface for reaching and grasping by primates, PLoS. Biol. 1 (2003) E42.
[11] T.M. Cover, J.A. Thomas, Elements of Information Theory, John Wiley & Sons Inc., 1991.
[12] M.D. Craggs, Cortical control of motor prostheses: using the cord-transected baboon as the primate model for human paraplegia, Adv. Neurol. 10 (1975) 91–101.
[13] O. Donchin, A. Gribova, O. Steinberg, H. Bergman, S. Cardoso de Oliveira, E. Vaadia, Local field potentials related to bimanual movements in the primary and supplementary motor cortices, Exp. Brain Res. 140 (2001) 46–55.
[14] O. Donchin, A. Gribova, O. Steinberg, H. Bergman, E. Vaadia, Primary motor cortex is involved in bimanual coordination, Nature 395 (1998) 274–278.
[15] S. Geyer, M. Matelli, G. Luppino, K. Zilles, Functional neuroanatomy of the primate isocortical motor system, Anat. Embryol. (Berlin) 202 (2000) 443–474.
[16] B. Graimann, J.E. Huggins, S.P. Levine, G. Pfurtscheller, Toward a direct brain interface based on human subdural recordings and wavelet-packet analysis, IEEE Trans. Biomed. Eng. 51 (2004) 954–962.
[17] T.J. Hastie, A. Buja, R.J. Tibshirani, Penalized discriminant analysis, Ann. Stat. 23 (1995) 73–102.
[18] E.C. Leuthardt, G. Schalk, J.R. Wolpaw, J.G. Jemann, D.W. Oran, A brain–computer interface using electrocorticographic signals in humans, J. Neural Eng. 1 (2) (2004).

[19] S.P. Levine, J.E. Huggins, S.L. BeMent, R.K. Kushwaha, L.A. Schuh, M.M. Rohde, E.A. Passaro, D.A. Ross, K.V. Elisevich, B.J. Smith, A direct brain interface based on event-related potentials, IEEE Trans. Rehabil. Eng. 8 (2000) 180–185.
[20] C. Mehring, J. Rickert, S. Cardoso de Oliveira, E. Vaadia, A. Aertsen, S. Rotter. Hints for a topographic map of tuning properties in primate motor cortex, in: Proceedings of the 1st International IEEE EMBS Conference on Neural Engineering, 2003.
[21] C. Mehring, M. Nawrot, A. Schulze-Bonhage, A. Aertsen, T. Ball, Decoding of movement direction from electrocorticographic (ECoG) recordings in human sensorimotor cortex—a potential basis for a brain–machine interface. 49. Ladislav Tauc Conf. in Neurobiology, Gif sur Yvette (France), 2003.
[22] C. Mehring, J. Rickert, E. Vaadia, S. Cardoso de Oliveira, A. Aertsen, S. Rotter, Inference of hand movements from local field potentials in monkey motor cortex, Nat. Neurosci. 6 (2003) 1253–1254.
[23] R.C. Oldfield, The assessment and analysis of handedness: the Edinburgh inventory, Neuropsychologia 9 (1971) 97–113.
[24] D.B. Percival, W.T. Walden, Spectral Analysis for Physical Applications: Multitaper and Convention, Cambridge University Press, Cambridge, UK, 1993.
[25] B. Pesaran, J.S. Pezaris, M. Sahani, P.P. Mitra, R.A. Andersen, Temporal structure in neuronal activity during working memory in macaque parietal cortex, Nat. Neurosci. 5 (2002) 805–811.
[26] G. Pfurtscheller, D. Flotzinger, M. Pregenzer, J.R. Wolpaw, D. McFarland, EEG-based brain computer interface (BCI). Search for optimal electrode positions and frequency components, Med. Prog. Technol. 21 (1995) 111–121.
[27] G. Pfurtscheller, B. Graimann, J.E. Huggins, S.P. Levine, L.A. Schuh, Spatiotemporal patterns of beta desynchronization and gamma synchronization in corticographic data during self-paced movement, Clin. Neurophysiol. 114 (2003) 1226–1236.
[28] G. Pfurtscheller, F.H. Lopes da Silva, Event-related EEG/MEG synchronization and desynchronization: basic principles, Clin. Neurophysiol. 110 (1999) 1842–1857.
[29] J. Rickert, S. Cardoso de Oliveira, E. Vaadia, A. Aertsen, S. Rotter, C. Mehring, Encoding of movement direction in different frequency ranges of motor cortical local field potentials, J. Neurosci. 25 (39) (2005) 8815–8824.
[30] J. Rickert, C. Mehring, S.C. de Oliveira, E. Vaadia, A. Aertsen, S. Rotter, Characteristics of directional tuning in local field potentials from monkey motor cortex. 49. Ladislav Tauc Conf. in Neurobiology, Gif sur Yvette (France), 2004.
[31] T. Satow, M. Matsuhashi, A. Ikeda, J. Yamamoto, M. Takayama, T. Begum, T. Mima, T. Nagamine, N. Mikuni, S. Miyamoto, N. Hashimoto, H. Shibasaki, Distinct cortical areas for motor preparation and execution in human identified by Bereitschaftspotential recording and ECoG-EMG coherence analysis, Clin. Neurophysiol. 114 (2003) 1259–1264.
[32] H. Scherberger, M.R. Jarvis, R.A. Andersen, Cortical local field potential encodes movement intentions in the posterior parietal cortex, Neuron 46 (2) (2005) 347–354.
[33] M.H. Schieber, M. Santello, Hand function: peripheral and central constraints on performance, J. Appl. Physiol. 96 (2004) 2293–2300.
[34] A.H. Schulze-Bonhage, H.J. Huppertz, R.M. Comeau, J.B. Honegger, J.M. Spreer, J.K. Zentner, Visualization of subdural strip and grid electrodes using curvilinear reformatting of 3D MR imaging data sets, AJNR Am. J. Neuroradiol. 23 (2002) 400–403.
[35] M.D. Serruya, N.G. Hatsopoulos, L. Paninski, M.R. Fellows, J.P. Donoghue, Instant neural control of a movement signal, Nature 416 (2002) 141–142.
[36] S. Shoham, E. Halgren, E.M. Maynard, R.A. Normann, Motor-cortical activity in tetraplegics, Nature 413 (2001) 793.
[37] D.M. Taylor, S.I. Tillery, A.B. Schwartz, Direct cortical control of 3D neuroprosthetic devices, Science 296 (2002) 1829–1832.
[38] D.J. Thomson, Spectrum estimation and harmonic analysis, Proc. IEEE 70 (1982) 1055–1096.
[39] C. Toro, C. Cox, G. Friehs, C. Ojakangas, R. Maxwell, J.R. Gates, R.J. Gumnit, T.J. Ebner, 8–12 Hz rhythmic oscillations in human motor cortex during two-dimensional arm movements: evidence for representation of kinematic parameters, Electroencephalogr. Clin. Neurophysiol. 93 (1994) 390–403.
[40] A. Treves, S. Panzeri, The upward bias in measures of information derived from limited data samples, Neural Comput. 7 (2004) 399–407.
[41] J.R. Wolpaw, N. Birbaumer, D.J. McFarland, G. Pfurtscheller, T.M. Vaughan, Brain–computer interfaces for communication and control, Clin. Neurophysiol. 113 (2002) 767–791.
[42] J.R. Wolpaw, D.J. McFarland, Control of a two-dimensional movement signal by a noninvasive brain-computer interface in humans, Proc. Natl. Acad. Sci. USA 101 (51) (2004) 17849–17854.